

SIMULATION OF ULTRASONIC FLOW POLISHING INSIDE THE MOLD CAVITY

Ting Lv, Yi Li*

College of Mechanical and Electrical Engineering, Soochow University, Suzhou 215006, China

*Corresponding Author E-mail: 505986788@qq.com

This is an open access article distributed under the Creative Commons Attribution License, which permits unrestricted use, distribution, and reproduction in any medium, provided the original work is properly cited.

ARTICLE DETAILS

Article History:

Received 12 November 2017
Accepted 10 December 2017
Available online 06 January 2018

ABSTRACT

The UDF program is written to simulate the cavitation characteristics of polishing media generated by ultrasonic vibration in the mold cavity based on CFD. The simulation results reveal the motion state of polishing media in the mold cavity. On the foundation of detailed study, the optimum combination range of simulation process parameter settings are obtained to play a guiding role for the surface ultrasonic polishing design and development, involving periodic regularity of absolute pressure and vapor fraction, the nonlinear effects of under-relaxation factors to simulation results.

KEYWORDS

Mold cavity, cavitation, ultrasonic polishing, polishing media

1. INTRODUCTION

With the continues development of the mold industry as well as its increasing market demands, the artificial treatment on mold surface will be unable to meet development requirements. Based on a study, there have been a number of other techniques used in mold polishing in addition to the traditional manual mechanical polishing methods on the market, and ultrasonic polishing method is one of the classic polishing methods, which is mainly used in the processing of brittle materials, round hole-type hole, cavity nesting and micro holes etc, shown in Figure 1 [1,2]. It is that ultrasonic polishing can be applied to many complex shaped cavity walls and the tool head for using in the ultrasonic polishing process can be made in soft materials or different shapes to adapt the mold cavity. However, this ultrasonic polishing technology for fluid movement in the field of ultrasonic vibration is still needed further study and this dissertation will study the basic theory in a novel polishing process for dies and molds. Ultrasonic cavitation generated by high-frequency ultrasonic transducer is investigated by theoretical analysis and numerical simulation so as to improve polishing efficiency and acquire reliable product quality.

2. NUMERICAL SIMULATION OF MODEL SELECTION

Establishing the model calculation region shown in Figure 2; Mixture model in multiphase flow [3,4]; Standard $k-\epsilon$ model in turbulence model; tool head end face used for the moving boundary; export conditions for the pressure outlet; the density of polishing abrasive media is 1100 kg/m^3 ; dynamic viscosity coefficient is $0.06 \text{ Pa}\cdot\text{s}$. UDF program is loaded to fluent dynamic grid settings, custom functions as follows [5,6]:

```
#include "udf.h"
extern "C" {
    DEFINE_CG_MOTION(function0,dt,vel, omega, time, dtime)
    time, dtime)
    {
        AFX_MANAGE_STATE(AfxGetStaticModule State());
```

```
real a, f, pi;
real y, w;
pi=3.141592653;
a=0.00002;
f=20000;
w=2*pi*f;
vel[1]=w*a*cos(w*time); }
```

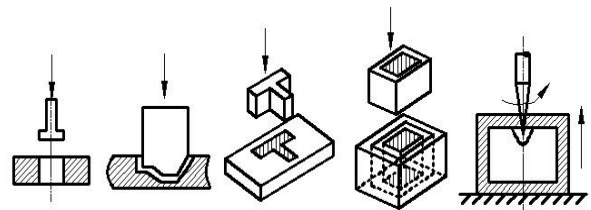


Figure 1: Different kinds of mold cavity.

Wherein, time of ultrasonic vibration time, vel refers to the speed in the vertical direction.

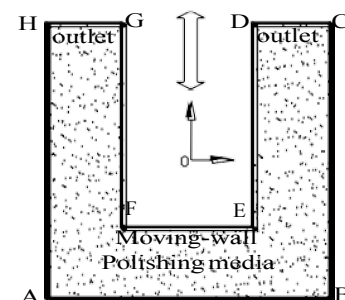


Figure 2: Simplified model of mold cavity.

3. SIMULATION PARAMETER SETTINGS

In Fluent simulation, the under-relaxation factors are crucial to be set [7,8], it is related to the phenomenon of turbulence and cavitation generation. Study showed since the mixture converges more difficult, it is not easy to converge in the case of relatively large convergence factors [9]. Five different groups of under-relaxation factor values are compared to each other in order to get a more accurate simulation results, shown in Table 1.

Table 1: Under-relaxation factors settings.

Under-Relaxation Factors	1	2	3	4	5
Pressure	0.1	0.3	0.3	0.3	0.3
Density	1	1	0.7	0.7	0.7
Body Forces	1	1	0.7	0.7	0.7
Momentum					
Vaporization	0.1	0.1	0.1	0.01	0.01
Mass Turbulence	0.1	0.1	0.1	0.001	0.001
Kinetic Energy					
Turbulence	0.8	0.8	0.8	0.8	0.2
Viscosity	0.8	0.8	0.8	0.8	0.2

In these five groups simulation in mold cavity, other parameters are the same in addition to the under-relaxation factors. Fluent solver is taken the steps of 1.0-E05s, 30 iterations, 100 steps are calculated each time to obtain the vapor profile inside the mold cavity shown in Figure 3.

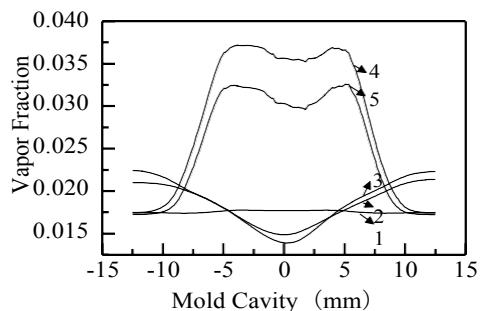


Figure 3: The distribution of vapor fraction in the mold cavity.

Three change trends can be seen from Figure 3 and there are differences in the same kind of curve fluctuations. Among them, the vapor fraction of group one is stable relatively and the content is very low. It is considered to be no vaporization occurs. The magnitude of group two and group three is closer, but the vapor fraction of two groups is nearly zero in the middle of the flow field because of the bubble collapse. Group four is similar with group five, but the vapor fraction of group four is a little higher than group five. In contrast, group two and three with respect to convergence is easier and more prone to vaporize than group one. The occurrence time of vaporization in group four and five is delayed compared to group two and three. As can be seen, the vaporization is effected by pressure coefficient sharply. A relatively small density and body forces are set to improve the continuity of flow field calculation process. Momentum and vaporization mass have a large impact on vaporization phenomenon. Turbulence kinetic energy and turbulence viscosity have a period effect on vaporization result and turbulence.

After calculating the same time, the absolute pressure contour diagram is obtained by Tecplot from Fluent, the results shown in Figure 4.

As can be seen from Figure 4, the absolute pressure of group one is almost no change inside the flow field and cannot reach the vaporization requirements. The absolute pressure of group two and

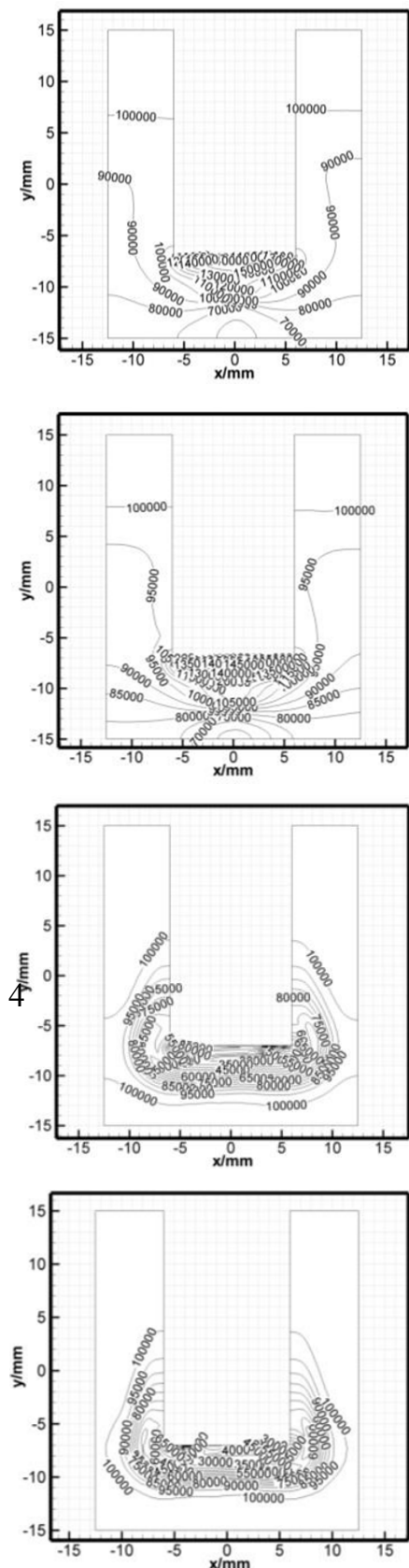
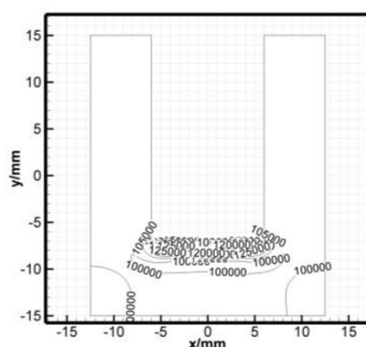


Figure 4: Contour pressure distribution.

three is produced a significant change and the pressure value stratification is obvious. In addition, it is visually shown that the distribution of the pressure is invalid in group four and five, the change of pressure is concentrated in the vicinity of the tool head, which the vibration of the tool head does not make up the whole flow field vibration. It is a serious deviation from the actual situation. Therefore, group two and three is more reasonable and able to meet the demands of reality under the comparison.

4. THE SIMULATION RESULTS AND APPLICATIONS

To study the effect of cavitation on ultrasonic polishing, no cavitation and cavitation should be compared in the flow field [10].

4.1 No Cavitation in the Flow Field

The calculation steps in the simulation are previous settings. As can be seen from Figure 5, the absolute pressure and vaporized bubbles have a clear regularity in the process of change of the ultrasonic vibration. Since the frequency of the tool head vibration is 20 kHz, the oscillation period is 0.5×10^{-4} s, so six cycles are ran within 0.3ms. At the same time, negative pressure appears in the flow field. Positive and negative amplitude is great and reach nearly 0.2 Mpa and -0.3 Mpa. The appearance of negative pressure makes partial pressure within the polishing medium below the saturation vapor pressure of the liquid, which is the condition of cavitation generated by ultrasonic vibration.

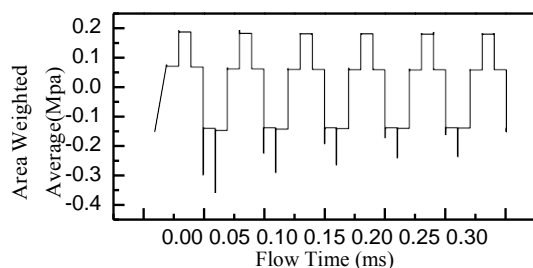


Figure 5: The absolute pressure curve around the moving-wall.

The velocity variation of the moving boundary shown in Figure 6, taking into account simulation error, the amplitude of the velocity is 2.5 m/s. According to the formula [11]:

$$v_{\max} = 2\pi fA \quad (1)$$

The vibration amplitude of polishing medium is $19.9 \mu\text{m}$ and it is approximately equal to ultrasound amplitude.

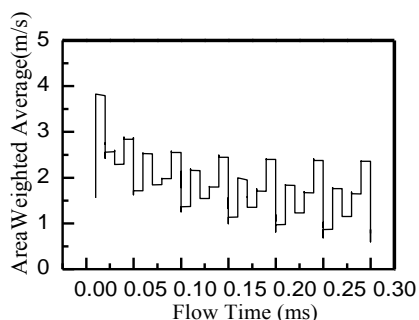


Figure 6: The velocity curve around the moving-wall.

Without the addition of cavitation model, the simulation process is only polishing action of abrasive particles in the polishing medium of the mold cavity. From Figures 7 and 8, it can be seen that the abrasive velocity of the ultrasonic vibrations under the bottom is about 0.3 m/s, the velocity around the inner wall of the mold cavity shaped polishing is 0.25 m/s, but the abrasive polishing rate near the mold cavity shaped corners is relatively small.

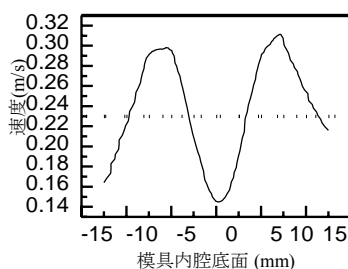


Figure 7: The abrasive velocity in the bottom.

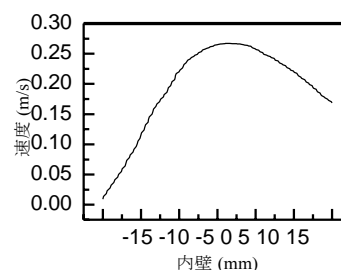


Figure 8: The abrasive velocity in the inner wall.

4.2 Cavitation in the Flow Field

The same time is calculated to obtain Figures 9 and 10. According to a study, the absolute pressure inside the polishing medium has undergone tremendous changes, negative pressure is no longer present [12-15]. The pressure amplitude is lower than that in no cavitation, but continues to show a cyclical absolute pressure change. At the same time, the vapor fraction has a corresponding change accompanied with the absolute pressure. The vapor fraction is reducing when the absolute pressure is increasing. On the contrary, the vapor fraction is increasing when the absolute pressure is reducing. And the maximum value of the absolute pressure is close to the standard, the minimum value of the atmospheric pressure is about 0.05 MPa. When the absolute pressure lower than the liquid flow field in saturated steam, it will have vaporization.

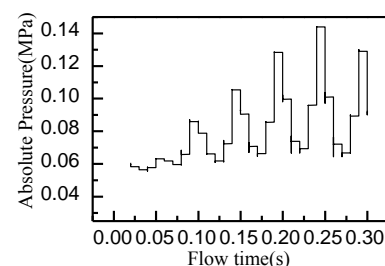


Figure 9: The distribution of absolute pressure.

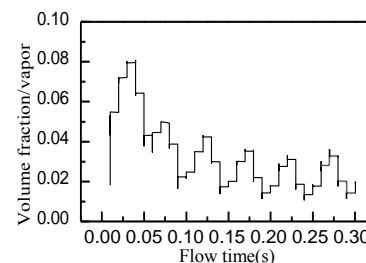


Figure 10: The distribution of vapor fraction.

As can be seen from Figures 11 and 12, the absolute pressure around the moving-wall is higher than both edges of the intermediate region. The flow direction of the liquid is up and down by ultrasound vibration, whereby the pressure difference creates a larger space "swirl." In addition, the flow field near the bottom forms a new turbulence to achieve the abrasive polishing to the mold under ultrasonic vibration effect.

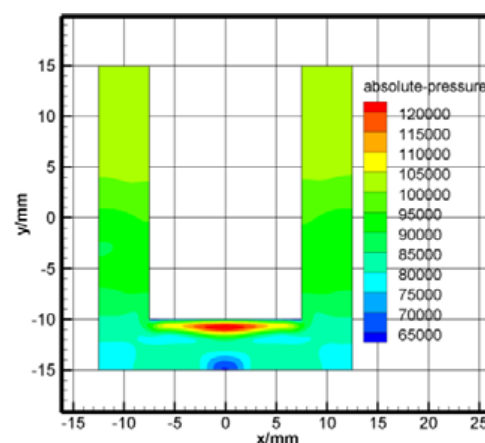


Figure 11: The distribution of the absolute pressure in the flow field.

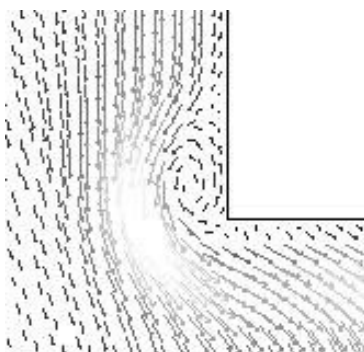


Figure 12: The velocity vector of abrasive around tool head.

From Figures 13 and 14, the speed of the abrasive particles around the inner wall of the mold cavity is up to 0.2 m/s or more, while the speed in the bottom region reaches 0.45 m/s. It is shown that the ultrasonic polishing can be used for mold cavity and reaches reliable polishing effects. Compared to simulation without cavitation model, the polishing rate is significantly increased after adding cavitation model in the flow field. It can be described that the generated ultrasonic cavitation during polishing can enhance polishing abrasive grains.

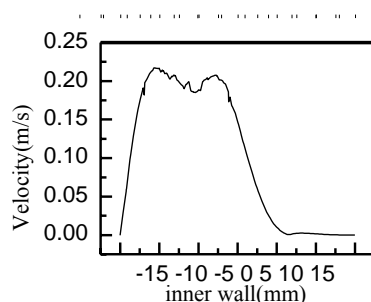


Figure 13: Abrasive velocity of inner wall.

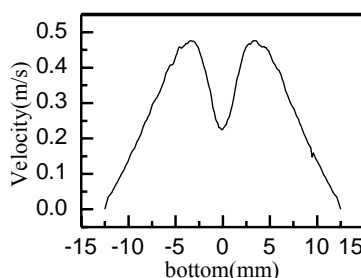


Figure 14: Abrasive velocity of the bottom.

[4] Petkovsek, R., Mocnik, G., Mozina, J. 2007. Measurements of the high pressure ultrasonic wave and cavitation bubble by optodynamic method, *Fluid Phase Equilibria*, 256, (1-2), 158-162.

[5] Shen, L. 2011. Numerical simulation of the flow field Induced by vibrating surface in the application of Ultrasonic cavitation, in Beijing: Tsinghua University.

[6] Kong, W., Cang, D.Q., Wang, W.B. 2011. Numerical simulation of macroscopic characteristics of ultrasonic cavitation in steel liquid, *Computer Application*, (2), 49-53.

[7] Merouani, S., Hamdaoui, O., Rezgui, Y. 2013. Effects of ultrasound frequency and acoustic amplitude on the size of sonochemically active bubbles-Theoretical study, *Ultrasonics Sonochemistry*, 30, (3), 815-819.

[8] Petkovšek, R., Močnik, G., Možina, J. 2007. Measurements of the high pressure ultrasonic wave and the cavitation bubble by optodynamic method, *Fluid Phase Equilibria*, 256, (1-2), 158-162.

[9] Qiao, Y.Z., Yin, H., Li, Z.P., Wan, M. 2013. Cavitation distribution within large phantom vessel and mechanical damage formed on surrounding vessel wall, *Ultrasonics Sonochemistry*, 20, (6), 1376-1383.

[10] Komarov, S., Oda, K., Ishiwata, Y., Dezhkunov, N. 2013. Characterization of acoustic cavitation in water and molten aluminum alloy, *Ultrasonics Sonochemistry*, 20, (2), 754-761.

[11] Ichida, Y., Sato, R., Morimoto, Y., Kobayashi, K. 2005. Material removal mechanisms in non-contact ultrasonic abrasive machining, *Wear*, 258, (1-4), 107-114.

[12] Hocheng, H., Kuo, K.L. 2002. Fundamental study of ultrasonic polishing of mold steel, *International Journal of Machine tools and Manufacture*, 42, (1), 7-13.

[13] Noltingk, B.E., Neppiras, E.A. 1950. Cavitation produces by ultrasonics, *Proceedings of the Physical Society. Section B*, 63, (9), 674-685, 1950.

[14] Singh, V.R., Lafaut, J.P., Wevers, M., Vincent, C., Baert, L. 2002. Transient cavitation and associated mechanisms of stone disintegration, *ITBM-RBM*, 21, (1), 14-22.

[15] Anton, Z., Robert, M., Matevz, D. 2015. Modeling cavitation in a rapidly changing pressure field-Application to a small ultrasonic horn, *Ultrasonics Sonochemistry*, 22, 482-492.



5. CONCLUSIONS

We apply mixture model and turbulence model to simulate acoustic cavitation for the first time. The energy generated by ultrasonic cavitation is discussed and it can enhance the abrasive polishing for the mold shaped cavity, resulting in more intense material removal. Moreover, there is no selectivity of cavitation. The distribution of cavitation is relatively stable, that is concentrated in the vicinity of the bottom center of the mold shaped cavity, while small around the inner wall and the edge of the area. The results show that the corresponding change in the velocity of the abrasive occurs according to the distribution of cavitation in the mold shaped cavity. To achieve a more precise machining effect in ultrasonic polishing, the influence of cavitation on abrasive material removal rate should be suppressed in order to strengthen the machining of abrasive itself to the workpiece.

REFERENCES

- [1] Hu, Y.S., Yu, M.J. 2004. Precision mold manufacturing process. Nanjing: Southeast University Press.
- [2] Jones, A.R., Hull, J.B. 1998. Ultrasonic flow polishing, *Ultrasonics Sonochemistry*, 36, (5), 97-101.